Influence of Chemical Composition and Pre-deformation on the Age-Hardening Response of Al-Mg-Si Alloys

A. Wimmer

Abstract

AlMgSi (6xxx) alloys are widely used in the lightweight construction of automotive structures. In addition to light weighting, the recycling of aluminum alloys plays an important role for the optimization of the carbon footprint in the automotive industry. On the one hand, optimized AlMgSi alloys require a narrow tolerance window, both for chemistry and process parameters, and on the other hand, increasing recycling rates are a challenge to achieve a defined chemistry. In this work, the influences of alloy chemistry, grain size, pre-deformation and heat treatment parameters such as quench rate and time/temperature profiles were analyzed. 20 different AlMgSi alloys, both with and without Cu, quench rates from 500 K/min to 30,000 K/min and ageing procedures including and excluding pre-deformation and natural ageing were systematically examined. For the alloy 6082 (AlMgSiMn) yield strength values above 400 MPa and elongation to fracture values exceeding 20% were measured.

Keywords

Aluminum • Age hardening • Impact extrusion • Carbon footprint • Thermomechanical processing

Introduction

The traditional process steps for age hardenable aluminum alloys (e.g. 6XXX-T6 alloys) are:

1. Melting, casting and homogenization (~550 °C [1, 2])
2. Solution heat treatment (SHT, ~550 °C [3])
3. Water quench
4. Natural ageing (NA)
5. Artificial ageing (AA, 150–250 °C [4]).

Dependent on the manufacturing process route, there is a deformation between process steps, e.g. after step 1 in the case of cold forging (impact extrusion) or between steps 2 and 3 in the case of traditional forging. However, new production technologies use a deformation step between step 3 and 5 (cold deformation of the water quenched state, with or without natural aging, resulting in 6082-T8 condition) or a deformation step after step 5 (cold deformation of the T6 state, resulting in 6082-T9 condition).

During melting and casting, the chemical composition of the alloy is set. Furthermore, the hydrogen content and initial grain size are influenced by melting and casting parameters. During Solution Heat Treatment (SHT), all elements, which dissolve below the solidus temperature (in the case of 6XXX alloys magnesium (Mg), silicon (Si) and copper (Cu)), form a solid solution. This solid solution is frozen during water quenching, resulting in a supersaturated solid solution. Ultimately, these dissolved elements precipitate during natural and/or artificial aging. It is not the nominal chemical composition, which defines the achievable hardness; rather it is the level of elements, which can be kept in supersaturated solid solution after the solutionizing and quenching processes.

In a previous study [5], different 6XXX alloys had been analyzed in a pre-deformed T8 and T9 state. In the initial experiments, the pre-deformation was not isothermal (temperature increase due to deformation energy up to 250 °C). This led to dislocation depletion and softening during deformation, disguising the real hardening potential.

Consequently, in the present study, the hardening potential of isothermal pre-deformation and the interaction with natural and artificial aging parameters have been analyzed. Additionally, the effects of chemical composition and quench rate were examined. Finally, the influence of the aging parameters and surface condition on corrosion properties was studied.

A. Wimmer (✉)
Neuman Aluminium Industries, Werkstraße 1, 3182 Marktl, Austria
e-mail: alexander.wimmer@neuman.at

A. Tomsett (ed.), *Light Metals 2020*, The Minerals, Metals & Materials Series,
https://doi.org/10.1007/978-3-030-36408-3_57

Experimental Details

In this study, more than twenty 6XXX alloys were analyzed, of which seven are presented here in detail (Table 1). Samples in the as-cast state were homogenized and solution heat-treated at 540 ± 10 °C for 1 h. Different quench-rates were realized along with different water quench temperatures, ranging from 20 to 100 °C. Samples were naturally aged between 10 min (minimum transfer time between quench and artificial aging, respectively between the quench and the hydraulic press in experiments with pre-deformation) and 1 week at 20 ± 5 °C. Isothermal cold deformation was performed at 20 ± 5 °C with a strain rate of approx. 0.1 s^{-1} in a hydraulic press, the temperature increase was <10 °C during deformation. Artificial aging (AA) was performed at −20, 20, 80 and 160 °C up to 360 h. Hardness tests were performed on a "KB Prüftechnik" hardness tester and tensile tests were performed with flat tensile specimens on a "Zwick Universal Prüfmaschine Z100". For corrosion testing (PV1113 intergranular corrosion test (IGC)) the samples were ground, cleaned and 120 ± 5 min exposed to the etchant, consisting of deionized water with 2.3% HCl and 1.8% NaCl. In the areas where the strongest intergranular corrosion was visible with the microscope, metallographic specimens were prepared and depth of the corrosion cracks measured.

Results and Discussion

Influence of Chemical Composition and Elements in Solid Solution on Mechanical Properties

The peak hardness (T66 condition, peak-aged condition) of the analyzed alloys as a function of the total content of soluble elements (Mg, Si and Cu) in wt% is shown in Fig. 1. It should be noted, there is only an empiric relation between the content of soluble elements and the peak hardness, as with different ratios between Mg, Si and Cu different types of precipitations are formed. Cu levels as low as 0.01 at.% may change the atomic structure of precipitates significantly [6]. Furthermore, for a more detailed analysis, the content in at.% should be used, as the number of atoms is the relevant factor in precipitation formation. However, in most cast-houses, wt% is used, and using at.% instead of wt% on the abscissa changes the graph only slightly (due to the difference in atomic weight of the elements). Finally, it is important to note, that 6061 is significantly stronger than expected based on the Mg, Si and Cu content. This can be explained by the much stronger effect of Cu (resulting in a different kind of Cu-containing precipitates) compared to Mg and Si.

The hardness in condition T66 is defined by the content of alloying elements in the solid solution after quenching and not on the nominal chemical composition. To achieve maximum hardness, all Mg, Si and Cu has to dissolve during SHT. Secondly, quenching from > 500 to < 200 °C has to be fast enough to freeze all elements in solid solution. The threshold for a high-alloyed 6082 (6082↑) is approx. 15 s, corresponding to a cooling rate of 1,200 K/min. For lower alloyed 6XXX alloys (e.g. 6060, 6063, 6005) a lower cooling rate is sufficient, because the "force" to precipitate elements is weaker.

Age-Hardening Response Without Pre-deformation

Figure 2 shows the age-hardening response of different 6XXX alloys for aging temperatures between −20 and +160 °C and for aging times up to 320 h. As expected with increasing content of alloying elements (Table 1 and Fig. 2), the hardness/strength in the as-quenched state increases, which is in good accordance with calculations based on [7], indicating that during SHT all soluble alloying elements (Mg, Si and Cu) were dissolved and kept in solid solution during quenching.

At −20 °C (circles in Fig. 2) there is minimal hardness increase until 320 h, indicating very little clustering/precipitation. For 6063 (Fig. 2b) there is an increase in hardness after 100 h at −20 °C (Fig. 2b). At +20 °C (room temperature storage, diamonds in Fig. 2), all

Table 1 Chemistry of the used alloys [wt%]. The signs (↓, ↑) indicate the level of the total magnesium, silicon and copper content (Mg + Si + Cu), which is shown in the last row, e.g. 6060↓ is a low alloyed 6060 alloy, 6060↑ is a higher alloyed 6060 alloy

Alloy	Si	Fe	Cu	Mn	Mg	Cr	Mg + Si + Cu
6060↓	0.46	0.23	0.01	0.05	0.35	0.01	0.82
6060↑	0.47	0.23	0.02	0.05	0.38	0.01	0.87
6063	0.59	0.23	0.01	0.06	0.49	0.01	1.09
6005	0.63	0.20	0.04	0.16	0.61	0.01	1.28
6082↓	0.92	0.20	0.04	0.52	0.69	0.16	1.65
6082↑	1.20	0.23	0.08	0.54	0.81	0.18	2.09
6061	0.80	0.28	0.34	0.13	1.00	0.12	2.14

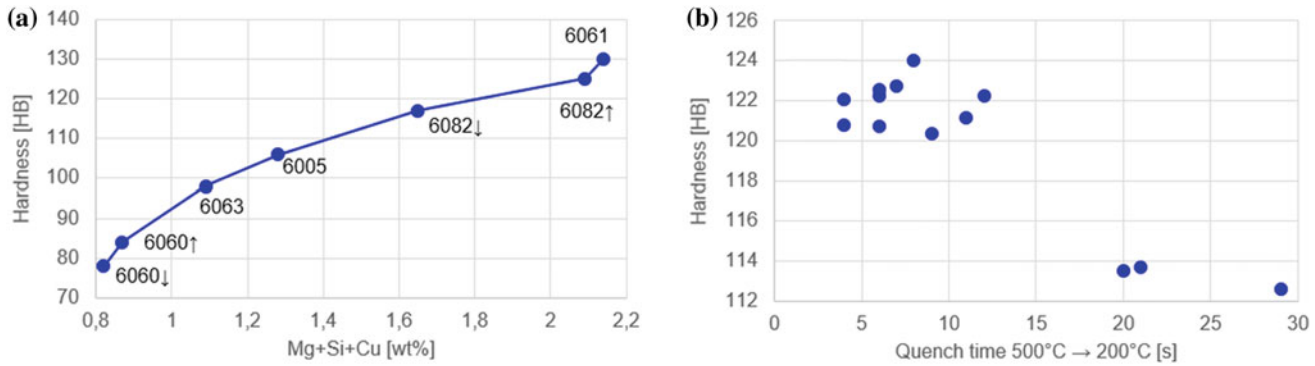

Fig. 1 **a** Hardness of different 6XXX-T66 alloys as a function of Mg, Si and Cu content, the Cu content of 6061 increases the hardness significantly compared to 6082↑. **b** Hardness of 6082↑-T66 alloy as a function of quench rate after solutionizing

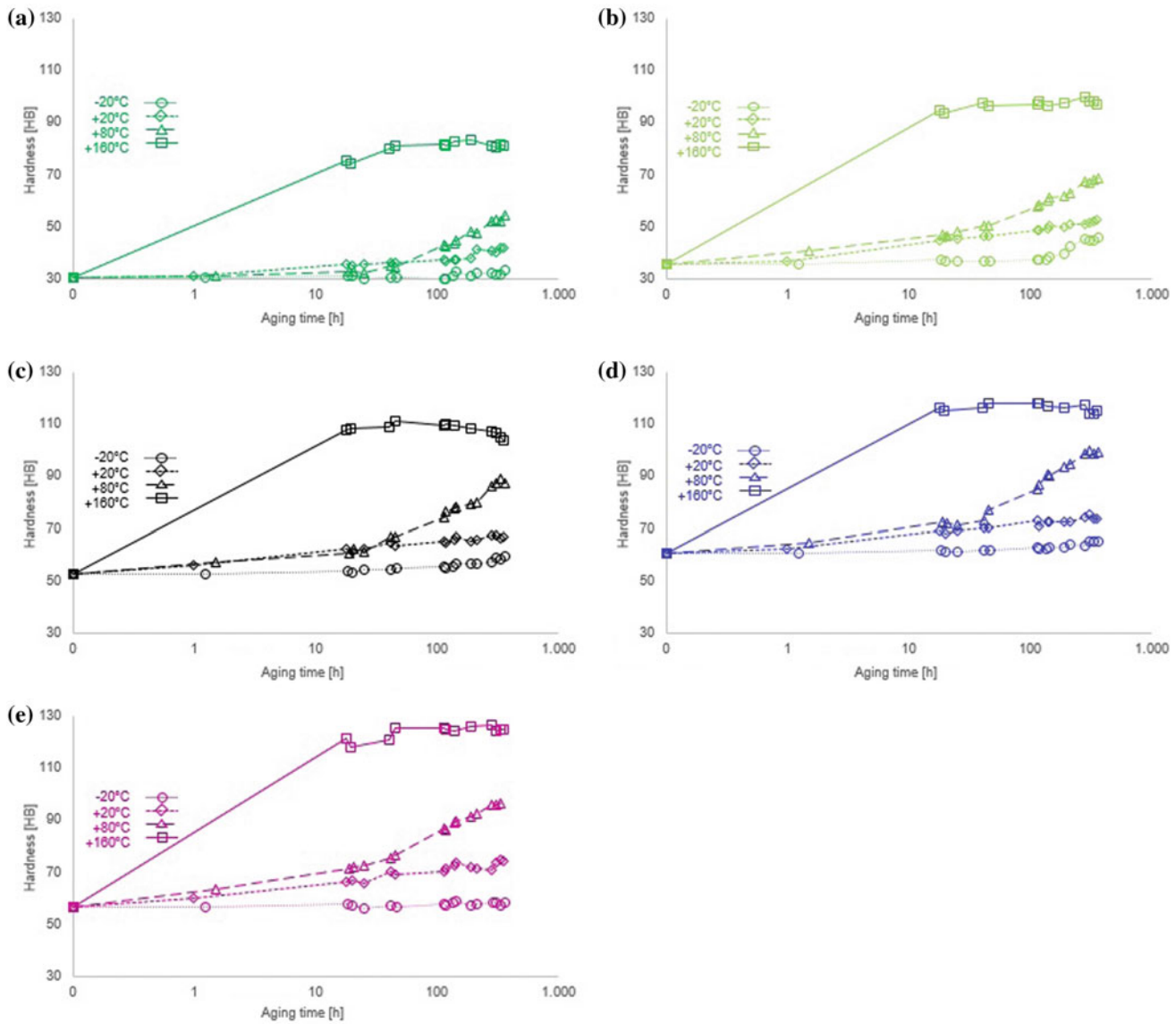

Fig. 2 Hardness of undeformed 6XXX-T6 alloy as a function of aging parameters and alloy composition. **a** 6060↑, **b** 6063, **c** 6082↓, **d** 6082↑ and **e** 6061

alloys show significant natural aging with a hardness increase of ~15 HB after 320 h. At +80 °C (pyramids in Fig. 2), all alloys show a hardness increase of ~50% compared to the hardness in the as-quenched state.

Interestingly, for 6060↑, the hardening response at +20 °C is faster than at +80 °C in the first 35 h (Fig. 2a). A possible explanation could be the dissolution of clusters, which were formed during quenching. At 160 °C (open rectangles in Fig. 2) all alloys reach peak hardness after 20–40 h. 6082↓ (Fig. 2c) and 6082↑ (Fig. 2d) show a decrease of hardness after 40 h, whereas 6060↑, 6063 and 6061 (Fig. 2e) remain stable at the peak hardness until 320 h. This indicates that Cu-free high-alloyed alloys (6082) are prone to over-aging compared to low-alloyed alloys (6060↑, 6063) and Cu-containing high-alloyed alloys (6061). In low-alloyed alloys, the "pressure" for cluster formation is lower, as the content of elements in the solid solution is lower. In Cu-containing high-alloyed alloys, Cu slows down the cluster/precipitation kinetics.

Figure 3 shows the elongation to fracture as a function of natural aging time and artificial aging parameters. The TEM inserts in Fig. 3 show the precipitation free zones (PFZ) at the grain boundaries with a thickness, dependent on the aging parameters, up to 100 nm. With increasing aging temperature and time, the elongation to fracture decreases. However, when the aging temperature exceeds 200 °C, which is typically not used in industrial processes due to the low hardening potential, the elongation to fracture increases with longer aging times. This can be explained by the difference in strength of the PFZ and matrix. In the peak-aged condition, the difference in hardness (ΔH) reaches its maximum of ΔH ~ 90 HB due to the low strength of the PFZ (consisting of 99.7% pure aluminum [8] with H_{PFZ} ~ 30 HB) and the high strength of the matrix (H_{matrix} ~ 120 HB). Consequently, the deformation is located in the soft PFZ with low elongation to fracture values.

With decreasing difference in strength between the PFZ and matrix, the elongation to fracture increases. E.g. in the under-aged condition H_{matrix} can be as low as the hardness of the solid solution ($H_{matrix} = H_{SS}$ ~ 60 HB). In the over-aged condition H_{matrix} can be as low as the hardness of the soft annealed material ($H_{matrix} = H_{soft}$ ~ 40 HB). This results in a hardness difference (ΔH) going down to 10-30 HB, leading to a delocalization of deformation with higher elongation to fracture values. Consequently, it is expected that elongation to fracture values for aging temperatures below 200 °C will also increase in the severe over-aged condition. However, this has low importance for most industrial processes due to long aging times (≫50 h) and low strength levels.

Age-Hardening Response with Pre-deformation

Figure 4a shows the age-hardening response for pre-deformation immediately after quenching (10 min transfer time/natural aging), followed by artificial aging. A peak hardness of 130 HB is reached after 30–40 h at 120 °C. Figure 4b shows the age-hardening response for pre-deformation after 1 week of natural aging at room temperature (20 °C), followed by artificial aging. A peak hardness of 140 HB is reached after 30–40 h at 100 °C. However, it has to be mentioned that pre-deformation reduces the ductility and the elongation to fracture decreases from 12 to 15% in the T66 state to 6–10% in the T8 state.

For a traditional T6 process, natural aging has a negative effect on strength/hardness, as some of the soluble elements get lost in "bad" clusters, which are not transforming to β″

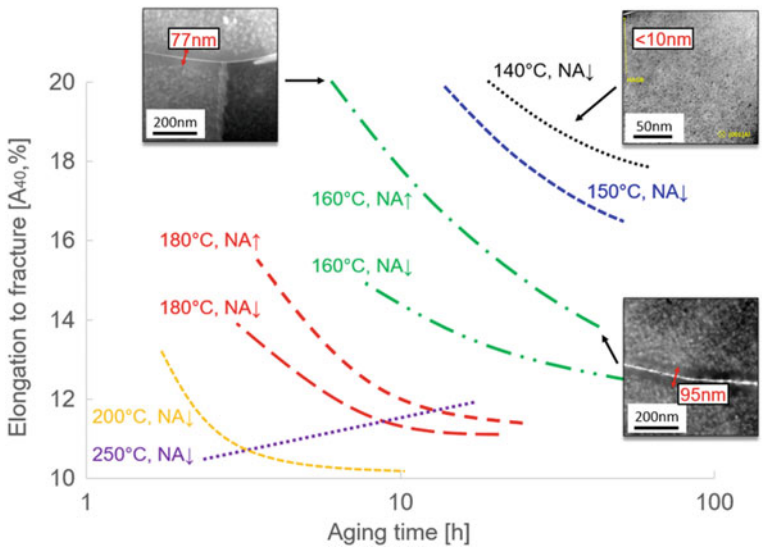

Fig. 3 Elongation to fracture as a function of natural aging time (NA↓: 10 min natural aging, NA↑: 1 week natural aging) and artificial aging temperature and time. TEM inserts are showing the precipitation free zone at the grain boundaries, increasing from <10 nm for 140 °C aging temperature up to ~100 nm for 160 °C aging temperature

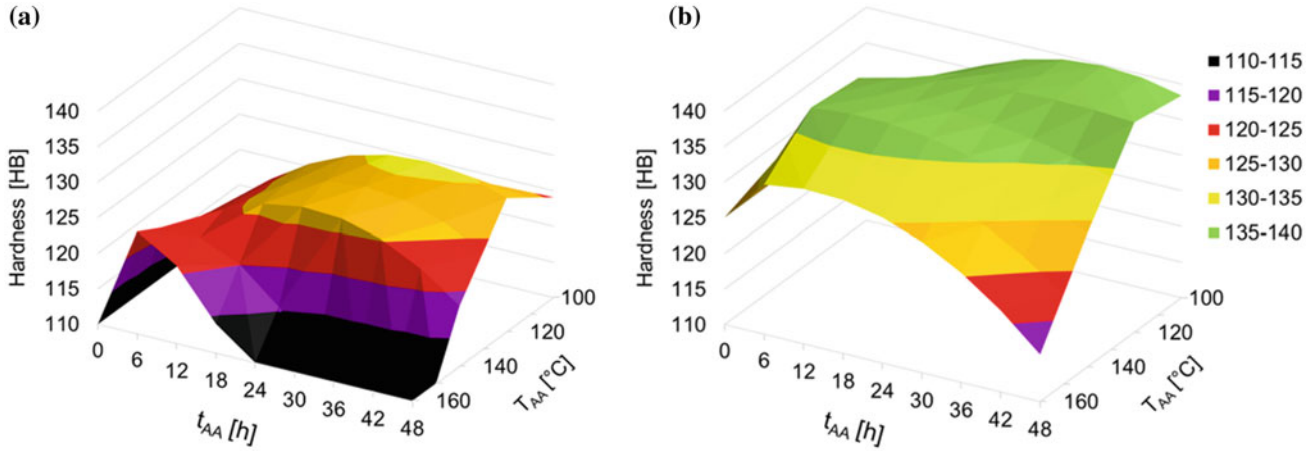

Fig. 4 Hardness of pre-deformed 6082↑-T6 alloy as a function of aging temperature and time. **a** 10 min natural aging between quenching and pre-deformation. **b** 1 week natural aging between quenching and pre-deformation

particles during artificial aging and consequently not contributing to strength in the T6 state [9, 10]. However, these "bad" clusters, which are formed during natural aging, can "pin" the dislocations during deformation in a T8 process and therefore the work hardening/dislocation hardening effect is stronger for pre-aged materials. Overall, after a T8 process, the artificial aging temperature has to be kept low (e.g. 100–120 °C). If not kept at low temperature, dislocations heal faster than precipitation hardening happens, which is also well known for severe plastic deformation (SPD) processes [11].

Influence of Artificial Aging and Surface Condition on Corrosion Properties

The results of corrosion testing (PV1113 intergranular corrosion test (IGC)) are shown in Fig. 5. In the peak-aged

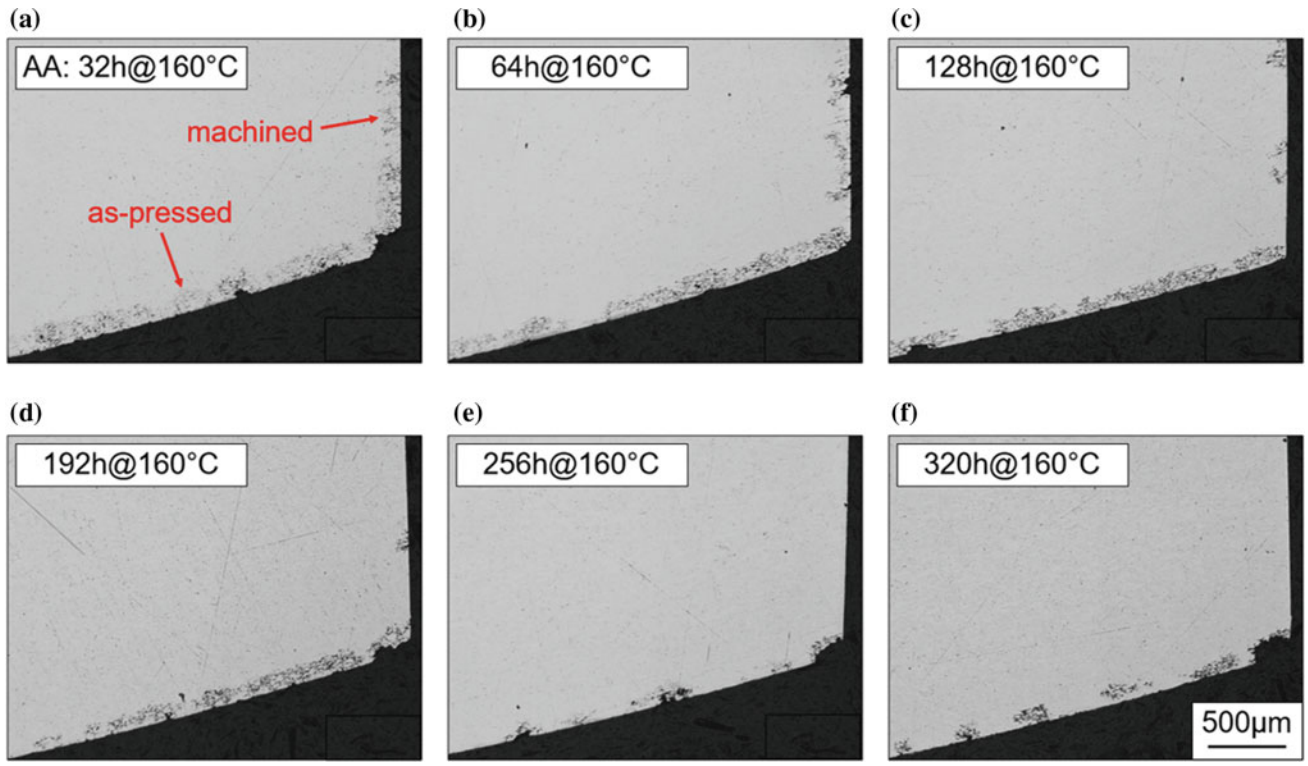

Fig. 5 Intergranular corrosion attack of high alloyed 6082 (6082↑) as a function of artificial aging time and surface condition

condition (T66, Fig. 5a) there is no significant influence between the as-pressed and machined surface, all surfaces show intergranular corrosion with a depth up to 250 µm. In the over-aged condition (T7, Fig. 5b–d) the corrosion attack decreases on the machined surface. In the severe over-aged condition (Fig. 5e, f) there is no corrosion on the machined surface any more. An explanation for this behavior is that impurities (e.g. residues and decomposition products of the metal containing lubricant) on the as-pressed surface initiate corrosion (electrochemical corrosion). Furthermore, machining generates a fine-grained surface layer due to deformations [12, 13], which delays intergranular corrosion attack due to longer corrosion pathways on the grain boundaries.

Conclusion

There is a tendency in the aluminum industry, especially the forging industry, to shift chemical alloy compositions to the upper limit of the standards. It has been shown that higher concentrations of alloying elements result in higher strengths only with a sufficiently high SHT temperature and adequate fast quenching in combination with tailor made artificial aging parameters. With this, hardness values of 130 HB, both for 6082↑ and 6061, can be reached, exceeding the limits of the standards (95 HB) by 40%. If the material is pre-deformed between natural and artificial aging, 6082↑ can reach a hardness of 140 HB and a yield strength exceeding 400 MPa.

It has to be considered that with higher contents of Mg, Si and especially Cu, the corrosion properties, in particular the resistance against intergranular corrosion, degrade. However, with the right heat treatment strategy (over-aging), combined with a surface treatment (machining), intergranular corrosion can be reduced significantly.

Acknowledgements The author thanks C. Graupp for performing the mechanical testing, JK Sunde and C.D. Marioara for the TEM analysis and B. Schwarz for the fruitful discussions. We are also grateful to the Austrian Research Promotion Agency FFG for their financial support (FFG project numbers 853869 and 872104).

References

1. Birol Y (2013) Optimization of homogenization for a low alloyed AlMgSi alloy. Materials Characterization 80:69–75
2. Zhao Q, Qian Z, Cui X, Wu Y, Liu X (2016) Influences of Fe, Si and homogenization on electrical conductivity and mechanical properties of dilute Al–Mg–Si alloy. Journal of Alloys and Compounds 666:50–57
3. Milkereit B, Starink MJ (2015) Quench sensitivity of Al–Mg–Si alloys: A model for linear cooling and strengthening. Materials & Design 76:117–129
4. Werinos M, Antrekowitsch H, Kozeschnik E, Ebner T, Moszner F, Löffler JF, Uggowitzer P, Pogatscher S (2016) Ultrafast artificial aging of Al–Mg–Si alloys. Scripta Materialia 112:148–151
5. Wimmer A (2017) Increasing strength and corrosion resistance of AlMgSi alloys by tailor-made thermomechanical processing, Light Metals 2017:433–438
6. Sunde JK, Marioara CD, Van Helvoort ATJ, Holmestad R (2018) The evolution of precipitate crystal structures in an Al-Mg-Si(-Cu) alloy studied by a combined HAADF-STEM and SPED approach. Materials Characterization 142:458–469
7. Engler O, Marioara CD, Aruga Y, Kozuka M, Myhr OR (2019) Effect of natural ageing or pre-ageing on the evolution of precipitate structure and strength during age hardening of Al–Mg–Si alloy AA 6016. Materials Science and Engineering A 759:520–529
8. Wimmer A (2018) Cold deformed aluminum parts for the automotive industry. Paper presented at the 7th Conference of Material Science and Engineering, Xian, China, 1–4 November 2018
9. Torsaeter M, Lefebvre W, Andersen SJ, Marioara CD, Walmsley J, Holmestad R (2010) Clustering behaviour in Al-Mg-Si alloys investigated by APT. Proceedings of the 12th International Conference on Aluminium Alloys (ICAA12):1385–1390
10. Marioara CD, Andersen SJ, Jansen J, Zandbergen HW (2003) The influence of temperature and storage time at RT on nucleation of the β″ phase in a 6082 Al–Mg–Si alloy. Acta Materialia 51:789–796
11. Dadbakhsh S, Karimi Taheri A, Smith CW (2010) Strengthening study on 6082 Al alloy after combination of aging treatment and ECAP process. Materials Science and Engineering A 527:4758–4766
12. Raof NA, Ghani JA, Haron CHC (2019) Machining-induced grain refinement of AISI 4340 alloy steel under dry and cryogenic conditions. Journal of Materials Research and Technology. https://doi.org/10.1016/j.jmrt.2019.07.045
13. Pan Z, Feng Y, Liang SY, Material microstructure affected machining: a review. Manufacturing Rev. 4(5):1–12